A native CO2-reducing bacterium: Discovery, implementation and interests

Azariel Ruiz-Valencia, Louis Cornette de Saint Cyr, Djahida Benmezianne, Eddy Petit, Loubna Karfane-Atfane, Héloïse Baldo, Valérie Bonniol, Sophie Pécastaings, Christine Roques, Delphine Paolucci-Jeanjean, et al.

Journal of CO2 Utilization 81 (2024) 102723

Contents lists available at ScienceDirect

Journal of CO2 Utilization

journal homepage: www.elsevier.com/locate/jcou

A native CO_2-reducing bacterium: Discovery, implementation and interests

Azariel Ruiz-Valencia [a], Louis Cornette de Saint Cyr [a], Djahida Benmezianne [a], Eddy Petit [a], Loubna Karfane-Atfane [a], Héloïse Baldo [a], Valérie Bonniol [a], Sophie Pécastaings [b], Christine Roques [b], Delphine Paolucci-Jeanjean [a], José Sanchez-Marcano [a], Marie-Pierre Belleville [a], Laurence Soussan [a,*]

[a] Institut Européen des Membranes, IEM – UMR 5635, Univ. Montpellier, ENSCM, CNRS, Montpellier, France
[b] Laboratoire de Génie Chimique (LGC), CNRS – Université de Toulouse, 4 allée Emile Monso, BP 84234, Toulouse 31432, France

ARTICLE INFO

Keywords:
Bacterial CO_2 reduction
S. maltophilia
Intracellular donor
Electrolysis
CO_2 removal

ABSTRACT

Stenotrophomonas maltophilia has been demonstrated herein to reduce CO_2 without any cofactor, photon or hydrogen (H_2) addition during reaction. *S. maltophilia* reduces $^{13}CO_2$ into ^{13}C-labeled formate in batch mode. Two intracellular enzymes are curently being considered for their ability to catalyze the CO_2 reduction reaction: a Fe-nitrogenase and a formate dehydrogenase (FeS-FDH). The reaction was intensified by implementing the bacteria in an electrolysis cell continuously fed with CO_2. In this configuration, CO_2 removal reached up to 25% *v/v* at 30°C and atmospheric pressure.

1. Introduction

Global warming is a major threat for humanity and greenhouse gas (GHG) emissions caused by human activities are reported to be a major cause for this [1,2]. Carbon dioxide (CO_2) rejection accounts for 75% of these anthropogenic GHG emissions, which are estimated to represent approximately 40 Gt per year [1]. Moreover, part of these emissions is relatively concentrated in CO_2, for example in plant chimneys, which could be treated and valorized by technologies that use CO_2 [1,3]. However, CO_2 is a very stable molecule (with C═O bonds exhibiting dissociation energy of 795 kJ.mol^{-1}) meaning that its activation is complex [4]. The ways for CO_2 activation can be either chemical (nucleophilic, thermochemical, electrochemical and photochemical) or biological (enzymatic, photosynthetic and microbiological), and many of these technologies are still being developed on a laboratory scale [3–6].

Carboxylation of carbon nucleophiles with CO_2 leads to carboxylic, carbonic and carbamic acids [4–7]. Thermochemical approaches consist either in producing syngas (that could serve as raw material for production of methanol, ammonia, or olefins) or in hydrogenating CO_2 to produce valuable products such as methanol or hydrocarbons [6,8]. Electrochemical conversion of CO_2 is in fact a CO_2 electrolysis which can be carried out either in liquid or gaseous phase [4,9–15]. The photocatalytic reduction of CO_2 can be carried out by using metallic catalysts where redox reactions occur to obtain solar fuels [4,15–18]. All these processes show several limitations, especially the need of transition or noble metals as catalysts and often the requirement of high temperatures or pressures.

Biological processes which activate CO_2 have the advantage of taking place in physiological conditions. Among these, the use of purified enzymes (carbon monoxide dehydrogenases, formate dehydrogenases and nitrogenases) has been reported, but this is still costly due to the need of extraction and purification steps, coupled with cofactor addition [4,19–22]. Photosynthesis, which occurs in plants and prokaryotes such as cyanobacteria and microalgae, can also lead to the production of fuels and gasoline by CO_2 fixation through the Calvin–Benson–Bassham (CBB) cycle [4,23–25]. Although these photosynthetic bioprocesses have already reached industrial levels, high surface areas and water consumption levels are still needed for cultivation, leading to competition with food crops. The use of hydrogenotrophic bacteria consequently appears as an attractive alternative. In particular, the species *Cupriavidus necator* (formerly named *Ralstonia eutropha*) is naturally able to use CO_2 and dihydrogen (H_2) to produce PolyHydroxyButyrate (PHB) [26,27]. Recently, *C. necator* strains were genetically modified to produce alcohols, alkanes, or alkenes [26,27], and expression of heterologous CBB cycle in some yeasts and *E. coli* was also carried out [28,29]. However, the latter microorganisms still suffer from poor growth rates and inefficient CO_2 fixation. Acetogenic bacteria and methanogenic archaea are

* Corresponding author.
E-mail address: laurence.soussan@umontpellier.fr (L. Soussan).

https://doi.org/10.1016/j.jcou.2024.102723
Received 30 October 2023; Received in revised form 6 February 2024; Accepted 27 February 2024
Available online 4 March 2024

also well-known hydrogenotrophic microorganisms catalyzing CO_2 fixation through the Wood–Ljungdahl Pathway (WLP) to obtain valuable products (methane, volatile fatty acids, alcohols…), but offer a low production rate [4,23]. Whatever the hydrogenotroph used, the need of costly and low solubility H_2 as an external electron donor constitutes the major drawback. Microbial Electrolysis Cells (MEC) in which H_2 could be produced *in situ* are of interest [30]. However, MEC does not currently solve the bio-availability limitation encountered with H_2.

The present study reports a new way that has recently been patented [31] to reduce CO_2 by the bacterial strain *Stenotrophomonas maltophilia*. This reduction reaction presents real assets since it can occur in the dark at 30°C and at atmospheric pressure, without any external addition of electron donors during the reaction. The implementation of this microorganism in a MEC – where H_2 production is not required - showed an improvement of the CO_2 reduction performance (*i.e.* CO_2 removal) by at least 20-times.

2. Materials and Methods

Chemicals, media, and gases

All chemicals were purchased from Sigma-Aldrich, France. For *S. maltophilia* culture, a Lysogeny Broth (LB) Miller solution was prepared at 25 g L^{-1}. Agar LB medium was also prepared by adding 15 g L^{-1} of microbiological agar to the LB broth. To assay CO_2 reduction, the reference reaction medium (RM) was composed of 20 mM phosphate buffer (pH 7.0 ± 0.1) and 5 mM $MgCl_2$ in deionized water. Alternatively, the reaction medium could be supplemented by 0.3 g L^{-1} Poly-HydroxyButyrate (PHB). All media were autoclaved (121°C, 20 min) before use. Concentrated hydrochloric acid (HCl) and sodium hydroxide (NaOH) pellets were used to prepare the electrode cleaning solutions. Chromatographic characterizations used HPLC grade benzoic acid, chloroform, lye (KOH), methanol (MeOH) and acetonitrile; and also PHB and sulfuric acid (97% *v/v*). Finally, different gases were employed: CO_2 (99.9%), $^{13}CO_2$ (99.9%), atmospheric air, nitrogen (N_2) at 99.995% and argon (Ar) at 99.999%. CO_2, N_2 and Ar were obtained from Linde Gas while labeled $^{13}CO_2$ was obtained from Sigma Aldrich. Gases were sterilized by filtration on a 0.22 µm-Teflon membrane (Sartorius Stedim, Germany). Helium (He) at 99.999% from Linde Gas was used as carrier gas in chromatographs.

Bacterial culture and suspension

The bacterial strain *Stenotrophomonas maltophilia* NCIMB 9203 was either isolated from a consortium with the methanotrophic bacterium *Methylosinus trichosporium* OB3b [32] (Appendice) or purchased from NCIMB (England) in freeze-dried form. The bacterium was cultivated on LB broth at 30°C in aerobic conditions. The strain was initially grown for 24 h on LB agar plates. After incubation, some of the plates were stored at 4°C for a maximum of 2 weeks before being sub-cultured on LB plates once again over 6 months at most. After 6 months, freeze-dried bacteria from NCIMB were used to restart the cultures. The rest of the plates were used to prepare fresh liquid cultures for the CO_2-reducing tests. Two successive liquid cultures were always carried out. Colonies formed on an LB plate were recovered with an inoculation loop to inoculate 100 mL of LB medium into a 250 mL Erlenmeyer flask. The flask was incubated for 24 h on an orbital incubator (Unimax 1010, Heidolph) at 30°C and 160 rpm, in aerobic conditions. The culture obtained was then used to inoculate LB medium in 1 L Erlenmeyer flasks (at 10% *v/v*). All 1 L-flasks were closed by breathable caps ensuring sterility. The subsequent culture was incubated for 24 h (at 30°C and 160 rpm) to reach an optical density at 600 nm (OD_{600}) of nearly 3.

A test was carried out at the end of each cultivation to check the absence of heterotrophic contaminations. For this, a sample of the liquid culture (10 µL) was spread onto an LB agar plate and incubated for 48 h at 30°C to examine the colony morphologies. For strain preservation, aliquots from the flask cultures were stored at −20°C with glycerol at 20% *w/w*.

At the end of the 1 L-flask culture, the culture medium was discarded by centrifugation at 4000 *g* for 20 min at 4°C and the cells were re-suspended in a same volume of the chosen reaction medium (RM with or without PHB). The bacterial suspension was then re-centrifuged at 3500 *g* for 20 min and 4°C. The recovered bacteria were then re-suspended in a minimal volume of reaction medium before being diluted in the reaction medium to reach an OD_{600} respectively of 10.3 ± 0.5 for the batch assays and 6.6 ± 0.3 for the fed-batch assays.

CO_2-reduction assay in batch mode

The bacterial suspension obtained was distributed in 60 mL-glass vials (6 mL per vial). Vials were closed with 20-mm chlorobutyl septa (Wheaton, USA) and sealed with aluminum caps (Gravis Orly, France). The atmosphere of the vial headspace was replaced by a sterile gaseous mixture. Different initial gaseous mixes were implemented to study the ability of *S. maltophilia* to catalyze CO_2 reduction: $^{13}CO_2$/atmospheric air (3:7 *v/v*), $^{13}CO_2/N_2$ (3:7 *v/v*) and pure $^{13}CO_2$. Once the headspace was filled with the gas mixture, vials were incubated at 30°C on a rotary shaker operated at 160 rpm. For each kinetics, identical vials were filled with the same bacterial suspension before being incubated. At different reaction times, a vial was taken to be analyzed to assess pH, OD_{600}, contamination, cell viability and the formate concentration. In some cases, NMR spectra were acquired and PHB concentrations were also assayed. The kinetics were reproduced at least twice each.

A $^{13}CO_2$/atmospheric air (3:7 *v/v*) mixture was assumed to initially contain 675 µmol of $^{13}CO_2$ (calculated on the basis of the perfect gas law at 30°C and atmospheric pressure), potentially convertible to 675 µmol of formate at a maximum and thus to a maximum final formate concentration of 112.5 mmol L^{-1} (since the liquid volume was fixed at 6 mL).

CO_2-reduction assay in fed-batch mode assisted by electrolysis

CO_2-reduction tests were also implemented in a homemade bio-electrolyzer. Two bioreactor sizes were employed: 100 mL total filled with 60 mL of bacterial suspension or 500 mL total filled with 400 mL of suspension (Schott® bottle, Duran, USA). The bacterial suspension was prepared according to Materials and Methods, Section 2. The screw cap was adapted with different inlet ports to hold the electrodes and the gas distributor. The electrochemical system was a classical 3-electrodes device (working electrode, reference electrode and counter electrode). A silicone seal was used to maintain the proofing of the system. The CO_2 was continuously fed through a 0.22 µm-Teflon gas filter (Sartorius, France) connected to a sintered steel sparger (10 µm pore size, Sigma Aldrich, France) that was submerged in the suspension. The gas distributor was placed next to the anode to evacuate the O_2 produced by water oxidation at the anode. The reactor was continuously fed with CO_2, Ar or a mixture CO_2/Ar (1:1 *v/v*) at various VVM, *i.e.* gas Volume per suspension Volume per minute (from 0.06 to 0.25 min^{-1} at 30°C and atmospheric pressure). A needle was placed in the cap to serve as gas vent and ensure pressure close to the atmospheric pressure inside the reactor; the needle outlet was connected to a 0.22 µm-Teflon gas filter to guarantee reactor sterility. A sterile magnetic stirrer was used to mix the suspension during the operation (at a rotation speed of 300 rpm).

The working electrode was a piece of 0.5 cm wide unpolished graphite screwed to a titanium wire; the dimensions of the graphite were fixed so that the ratio of the projected cathode surface to the suspension volume was 0.10 ± 0.01 m^2 m^{-3}. The graphite piece was cleaned before each experiment. It was first immersed 1 h in HCl 1.0 N in order to dissolve eventual organic compounds present on the graphite surface and then in NaOH 1.0 N for another 1 h to neutralize the residual surface acidity; it was then rinsed with sterile deionized water in sterile conditions. Finally, the graphite electrode was immerged overnight in 1 L of

sterile deionized water to remove any eventual NaOH residues. A large platinum grid (Good Fellow, UK) served as counter electrode; before use, the platinum grid was cleaned and disinfected by flame heating. The potentials were expressed in relation to an Ag/AgCl reference electrode (Radiometer analytical, France). The potential of the reference electrode implemented in the reactor was checked before and after each experiment against an Ag/AgCl electrode that was used for this purpose only. The electrodes of the reactor were connected to a potentiostat (Versastat 3, Ametek, USA). A chronoamperometry (CA) assay was carried out. For that, a cathodic polarization ($V_{polarization}$) was applied at the working electrode from the beginning of the experiment (the polarization potential ranging from −0.70 V to −1.00 V vs Ag/AgCl) and the current (I) was continuously recorded every 600 s. The temperature was maintained at 30 °C and the pH was measured over time. The pH appeared to be stable at 6.4 ± 0.2 when CO_2 was bubbled. Liquid samples were taken to assay formate. When CO_2/Ar was bubbled in the reactors, gas samples were collected at the outlets of the reactor in 22 mL-headspace sealed vials (Perkin Elmer, France); gases being flowed in the vials for at least 24 h before their collection. A blank (*i.e.* a bio-electrolyzer without bacteria) was always run simultaneously with the same inlet gas to assess the possible CO_2 losses through the reactor (due to solubilization and hydrodynamics) and distinguish them from CO_2 consumption by the reaction. Gas outlets were analyzed by GC-MS to determine the CO_2 removal (% v/v) by comparison to the blank reactor.

Bacterial characterizations during the tests

2.1. OD_{600} measurements

To easily characterize the bacterial concentration of the samples, a correlation given in Equation (1) was established between the optical density at 600 nm (OD_{600}) of the bacterial suspension and its concentration in dry cell mass based on six points, each reproduced twice:

[dry cell concentration] ($g_{dry\ cell}\ L^{-1}$) = 0.3035 x OD_{600} (-) Eq. (1)

The linear regression coefficient (R^2) of the correlation is 0.995. The OD_{600} of the bacterial samples were measured in a double beam spectrophotometer 7315 (Jenway, UK).

2.2. Counting of the cultivable cells

At the beginning and at the end of the CO_2-reduction tests, the cell cultivability was investigated. Determination was based on the ability of the bacteria to grow again in their native culture conditions (Materials and methods, Section 2). The concentrations of the bacterial samples were enumerated by the conventional plaque assay method (Colony Forming Units (CFU) counts). For this, the bacterial suspension sampled was diluted by decades in phosphate buffer 20 mM at pH 7.0 ± 0.1. One mL of each dilution was immediately spotted on a LB agar plate and incubated 48 h at 30°C to enable counting of the bacteria colonies, assuming that each colony stemmed from one initial bacterium. The counting was performed twice and the concentrations of bacteria in the suspension were calculated as the average of the number of colonies divided by the volume inoculated on the agar, with the corresponding dilution factor considered. The quantification limit was 25 CFU mL^{-1}.

2.3. Contamination tests

The bacterial samples were spread onto LB agar plates using a 10 μL inoculation loop; the plates were then incubated at 30°C for 48 h to check the morphology of the colonies and the absence of contamination.

2.4. 16S-rDNA and genomic DNA (gDNA) sequencing

16S-rDNA sequencing was carried out for strain identification. For consortia, strains corresponding to different colony morphologies were isolated by spreading on LB agar plates and 72 h of incubation at 30°C. For all cases, single colonies of pure culture were suspended in phosphate buffer that was centrifuged 5 min at 15.000 g and 4°C. The supernatant was then discarded, and the recovered pellets were sent for sequencing (Genoscreen, France). DNA was extracted and 16S-rDNA sequences were amplified using PCR, then sequenced by Sanger Sequencing. The sequences obtained were assembled using Sequencher v4.7 (Gene Codes Corp.) and then compared to the NCBI database using "Somewhat similar sequences (blastn)" in the BLAST tool of NCBI [33]. For quality control reasons, both positive controls (with *E. coli*) and negative controls (mix without bacteria) were realized.

gDNA sequencing was only carried out on a pure culture of S. maltophilia that was already used for CO_2 reduction tests. Samples for gDNA sequencing were prepared as for 16S-rDNA sequencing. gDNA was extracted, quantified, qualified, and then sequenced using Illumina® Mi-Seq technology. The reads obtained were filtered to remove noisy sequences (Minoche et al. [34]), and assembled using MEGAHIT v1.2.9 [35], with a minimum contig length of 1 kbp. Bowtie2 [36] was used to map the contigs and create the sample profile. The metagenomic workflow for anvi'o [37] was then used to visualize and manually bin the contigs. The binning was based on their sequence composition and differential coverage to obtain high quality Metagenome Assembled Genomes (MAG) with completion >90% and redundancy <5%. The taxonomy was estimated by using the single-copy core gene sequences and the GTDB database [38]. Finally, the contigs were annotated using KEGG [39], pfam [40] and COG [41].

Physicochemical analyses

2.5. pH measurements

pH was measured using a pH-meter C831 and a standard pH electrode SP21B (Consort, Belgium).

2.6. RMN analyses

Bacterial suspensions exposed to $^{13}CO_2$ were monitored by NMR ^{13}C analysis. For NMR analysis, 450 μL of the sample (bacterial suspension freshly recovered from the batch reactors) were put in a 5 mm NMR capillary tube with 50 μL of D_2O. The analyses were performed on an NMR BRUKER Avance III – 500 MHz – CryoProbe Helium for four hours. Different standards prepared in the reaction medium were independently analyzed by NMR to get the carbon spectra of these molecules. Sodium formate labeled with ^{13}C ($NaH^{13}CO_3$) was also analyzed. The lower detection limit of the NMR device is 6 mg L^{-1} of ^{13}C. NMR analysis can distinguish only the ^{13}C-isotope which is 1.1% abundant in nature with regards to ^{12}C.[32] Consequently, a concentration of non-labelled products of about 600 mg L^{-1} is necessary to be able to identify these compounds.

2.7. GC-MS analysis

PHB, formate and gases were assayed by gas chromatography coupled with mass spectrometry (GC-MS). GC-MS analyses were performed with a Clarus SQ-8S GC/MS (Perkin Elmer) system, equipped with a quadrupole mass selective detector based on electron impact (EI) operated at 70 eV. For PHB analysis, organic samples were directly injected in the GC. For formate and gases, samples were previously collected in 22 mL-headspace vials (Perkin Elmer) and mixed with reactants in the case of formate analysis. Headspace vials were then heated in a Turbomatrix HS16 autosampler (Perkin Elmer, USA) and the vial headspace was then injected into the GC. A DB-1 column (Agilent J&W, USA) was used for separation in the case of PHB analysis while an Rt-Q-Bond Plot (Restek, France) capillary column was used for formate and gas analyses. In all cases, the carrier gas was helium.

2.7.1. PHB assay. In some cases, the PHB concentration of the bacterial suspension implemented in the CO_2-reduction tests was measured along with the reaction kinetics. The PHB assay was based on PHB digestion followed by the analysis of the monomer (*i.e.* 3-hydroxybutyrate) by GC-MS [42,43]. Here, the bacteria were not lyophilized but just frozen before the PHB digestion step. Firstly 1 mL of the bacterial suspension was centrifuged at 10 000 *g* and room temperature for 15 min. The

recovered pellets were then frozen at – 20 °C until their analysis. The frozen pellets were firstly thawed at room temperature and digested for 3 h at 100 °C with 2 mL of methanol containing 0.5 M H_2SO_4 and 0.01 M benzoic acid plus 2 mL of chloroform. Afterwards, the samples were cooled, and 1 mL of deionized water was added to induce a phase separation. Aqueous phase was discarded and 2 μL of the organic phase were injected into the GC-MS. The helium flow rate was fixed at 32 mL min^{-1}. The oven temperature was programmed from 80°C for 1 min, up to 120°C at a rate of 10°C min^{-1}, the temperature was then increased up to 270 °C at a rate of 45 °C min^{-1}. The temperature of the injector was set at 200 °C and the split ratio was 30 mL min^{-1}. PHB standard was used to establish a calibration curve. The ratios between 3-hydroxybutyrate and benzoate specific peak areas evolved linearly with the different PHB masses introduced, with a linear regression coefficient $R^2 = 0.9865$, on the basis of 10 points, which were each reproduced twice. This linearity is consistent with the literature [42,43].

2.7.2. Formate assay. Analyses of formate (^{12}C and ^{13}C) were performed by GC-MS in the samples and their supernatants (obtained by sample centrifugation at 10 000 *g* for 10 min at 10°C). As formate is not volatile, a modified derivatization method based on the protocol described by Wallage *et al.* [44] was employed for its quantification. The method consists of heating and acidifying the samples to obtain the corresponding carboxylate (*i.e.* formic acid, $HCOO^-$) and carrying out a methyl esterification reaction by methanol (CH_3OH) addition. The balance of the reaction is given in Eq. (2):

$$HCOO^- + CH_3OH \rightarrow HCOOCH_3 + H_2O \quad (2)$$

Reaction products are the corresponding methyl ester (*i.e.* methyl formate, $RCOOCH_3$) and water (H_2O). In a headspace vial, 600 μL of the sample, 100 μL of an acetonitrile (CH_3CN) solution prepared in deionized water at 157.2 mg L^{-1}, 100 μL of concentrated sulfuric acid (97% *v/v*) and 100 μL of methanol were successively introduced in that order. Acetonitrile was used as the internal standard, whereas sulfuric acid and methanol were derivatizing agents. Headspace vials were heated at 100°C for 15 minutes in the Turbomatrix autosampler to complete the esterification reaction. The helium flow rate was fixed to 1.5 mL min^{-1}. The oven temperature was programmed from 40 to 150 °C at a rate of 10 °C min^{-1}. The temperature of the injector was set at 200 °C and the split ratio was 1:16. Standard sodium formate (NaHCOO) was used to establish calibration curves. The specific ions coming from methyl formate were detected by single-ion recording (SIR) mode. The specific *m/z* ratios of these ions (where m is the ion molar mass and z its charge) were respectively 60 (for unlabeled methyl formate) and 61 for methyl ^{13}C-labelled formate. Specific peak areas were normalized to the acetonitrile peak area and the area ratios were correlated to the standard concentrations. A linear correlation was found for methyl formate (either labelled or not), with a linear regression coefficient R^2 of 0.9845, based on 5 points (each reproduced twice). The method was validated through total formate assays by ionic chromatography (data not shown).

2.7.3. Gases. Gas compositions at the inlet and the outlet of bio-electrolyzers were characterized by GC-MS. Gas samples were collected in 22 mL-headspace sealed vial (Perkin Elmer, France). Argon was used as an internal standard. The vials were placed in the Turbomatrix autosampler and incubated 5 min at 75°C. Helium was flowed at a rate of 1.1 mL min^{-1}. The oven temperature was programmed as isothermal at 40 °C. The temperature of the injector was set at 200 °C and the split ratio was 1:100. Standards of CO_2 and argon were previously analyzed in a scan mode to identify their retention times and characteristic *m/z* ions. The scan range was established at between 4 and 50 Daltons. Further single-ion recording (SIR) analysis allowed increasing sensitivity in samples. Specific *m/z* ratios of 4 for helium, 40 for argon and 44 for CO_2 were obtained. Specific peak areas were normalized to argon peak area to obtain the area ratios. The relative difference between the area ratios measured in inoculated electrolyzer outlets and in the blank reactors (without bacteria) gave the real CO_2 removal (in % *v/v*) enabled by the bio-electrolyzer.

GC-MS analyses were confirmed by GC analyses coupled to a katharometer detector. These latter analyses were carried out with a GC Clarus 580 (Perkin Elmer, France). The inlet and the outlet of the bio-electrolyzer were respectively connected online to the GC injection loop (a 10-way valve). The injected gases were separated by two different columns in series, an Elite Plot Q (Perkin Elmer, France) and an Elite-GC GS Molesieves (Perkin Elmer, France). Helium was used as carrier gas at a flow rate of 20 mL min^{-1}. The oven temperature was increased from 40°C to 120°C at a rate of 4 °C min^{-1} to 70°C and then 9°C min^{-1} to 120°C. It was then maintained for 7 min at 120°C. The separated gases then passed through the katharometer detector for identification and quantification. A characteristic retention time was first determined for argon and CO_2. The CO_2 peak area was normalized by the argon peak area since argon is an inert gas. The area ratio obtained for the Ar/CO_2 mixture analysed was correlated to its CO_2 volume content. Calibration was established with standard gas mixtures of known compositions.

3. Results and discussion

Evidencing the ability of S. maltophilia to reduce $^{13}CO_2$

A previous study carried out at our laboratory showed that a consortium including the methanotroph *M. trichosporium* OB3b was able to reduce $^{13}CO_2$ into ^{13}C-labelled formate ($H^{13}COO^-$) [32]. This consortium was shown to be composed predominantly of *M. trichosporium* OB3b NCIMB 11131 and *S. maltophilia* NCIMB 9203 (Appendice); where *S. maltophilia* is known to be a Gram-negative and facultative anaerobic bacterium [45]. Both strains were consequently isolated and tested independently in batch mode with an initial gas mixture of $^{13}CO_2$/atmospheric air (3:7 *v/v*), the reference reaction medium (RM) and an initial bacterial concentration of 3.1 ± 0.2 $g_{dry\ cell}\ L^{-1}$. In this configuration, the reaction conditions were defined as the reference conditions. NMR characterizations were carried out on the bacterial suspensions along the kinetics to evidence the $^{13}CO_2$ assimilation and the consequent production of ^{13}C-labelled compounds likely to arise from $^{13}CO_2$ fixation and reduction. In the tested conditions, only *S. maltophilia* gave a positive result with the production of ^{13}C-labelled formate, as shown in Fig. 1.

Fig. 1 shows that two peaks were visible from the beginning (Fig. 1 A): one associated to $^{13}CO_2$ and the other to its ionized form, *i.e.* bicarbonate ions ($H^{13}CO_3^-$). Their chemical shifts correspond to 124.6 ppm and 160.2 ppm respectively. After 8 days of kinetics (Fig. 1B), a peak with a chemical shift corresponding to ^{13}C-formate (*i.e.* 170.9 ppm) appeared. It was observed that the addition of ^{13}C-formate standard (at a final concentration of 10 mg L^{-1}) to the sample led to an increase in peak amplitude confirming that this peak corresponds to ^{13}C-formate (data not shown). This peak was still present after 35 days of reaction (data not shown). No other compound than ^{13}C-formate was significantly detected by NMR spectroscopy, suggesting that formate arose from direct $^{13}CO_2$ reduction. Indeed, ^{13}C-formate has only one carbon at a lower oxidation degree than that of $^{13}CO_2$. Blanks carried out in the same conditions but without bacteria did not show any labelled compounds except $^{13}CO_2$ and $H^{13}CO_3^-$ (data not shown), confirming the role of the bacteria in the $^{13}CO_2$ reduction. The kinetics were repeated to check the ability of *S. maltophilia* to reduce CO_2, and only the peak corresponding to ^{13}C-formate (170.9 ppm) was again observed. In conclusion, *S. maltophilia* catalyzes CO_2 reduction and formate is the main product of this reduction reaction in batch mode.

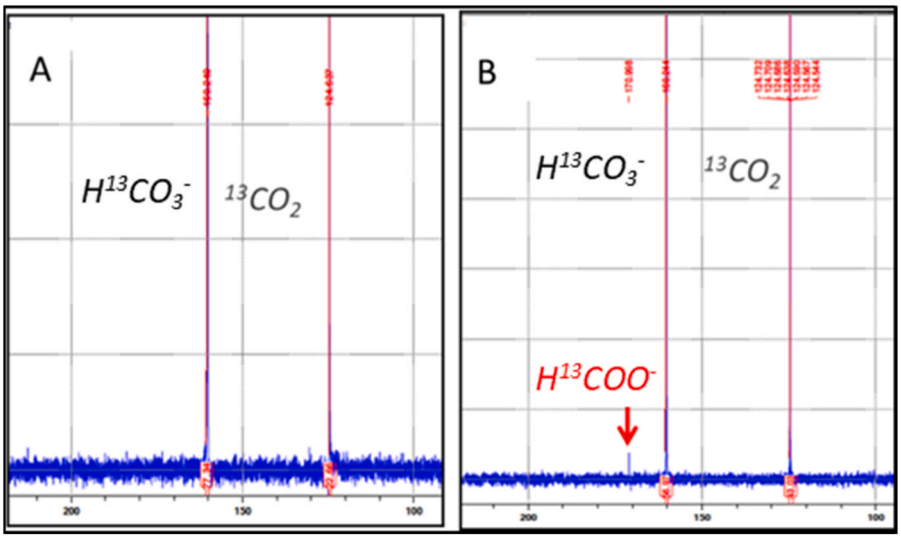

Fig. 1. $^{13}CO_2$ reduction test with *S. maltophilia* in batch mode: NMR spectra (A) at day 0 and (B) after 8 days reaction.

$^{13}CO_2$ reduction by S. maltophilia in batch mode in reference conditions: quantification and reproducibility assessment

Five independent trials were carried out in batch mode under reference conditions to assess the reproducibility of the bioprocess. For each trial, a new bacterial suspension of the isolated *S. maltophilia* was prepared from liquid cultures obtained by inoculating a fresh culture medium (as detailed in the Materials and Methods, Section 2). Trials were classified in chronological order, from A to E. Experiments D and E were launched at the same time from the same initial bacterial suspension. Between two CO_2 reduction tests, the biocatalyst was maintained on LB agar plates, except between experiments B and C, where the liquid bacterium culture was stored frozen at −20°C in glycerol 20% *w/w* during 4 weeks. The biomass concentration (by OD_{600} measurements and counting of viable cells), pH and formate production (by GC-MS measures) were monitored throughout the reaction. GC-MS measurements were carried out both on the whole bacterial suspension and on the associated supernatants after centrifugation.

Fig. 2 gives the evolution of ^{13}C-formate concentration assayed on the whole suspension and the cell dry mass concentration (OD_{600} measurements) during all $^{13}CO_2$ reduction trials, except for trial A for which the cell dry mass was not measured.

Independently of the kinetics, GC-MS analysis confirmed the ability of the isolated *S. maltophilia* to produce ^{13}C-formate from $^{13}CO_2$ (Fig. 2a). No production was observed in blanks (data not shown). In parallel, the sample supernatants assays did not show ^{13}C-formate during the kinetics, which suggests that the formate was produced and stored inside the cells. The bacteria can be thus considered to be the biocatalyst of the CO_2 reduction reaction resulting in formate production.

For all kinetics, a latency period was observed before the ^{13}C-formate was produced (Fig. 2a). However, the latency periods and the formate production rates differed between the different kinetics; the lag phases ranged from 5 to 25 days and the maximal ^{13}C-formate concentrations ranged from 50 to 280 μmol L^{-1} (Fig. 2a). Furthermore, the cell dry mass concentration exhibited a similar behavior between experiments (Fig. 2b). For all the runs, the cell concentration decreased from 3.1 ± 0.2 $g_{dry\ cell}$ L^{-1} to a stabilized value around 0.5 ± 0.1 $g_{dry\ cell}$ L^{-1}.

This result demonstrates cell lysis during reaction, but some bacteria were still present at the end of the reaction. A control carried out on the bacterial suspension at the end of the reaction confirmed that nearly 1.5 ± 0.4 × 10^5 CFU mL^{-1} of the bacteria were still cultivable and thus maintained a metabolic activity; the initial concentration being 6 ×10^9 CFU mL^{-1}. Both cultivability loss and cell death consequently occurred. This could result from the lack of natural nutrients and an energy source that exposes the cells to stressful conditions. It was notably reported that

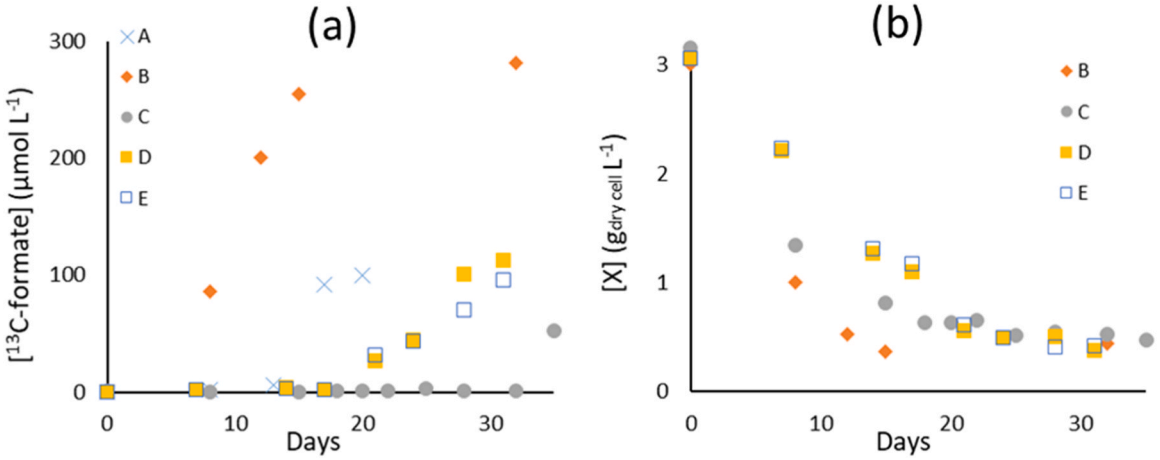

Fig. 2. $^{13}CO_2$ reduction trials carried out in batch mode in reference conditions: (a) ^{13}C-formate concentration (μmol L^{-1}) and (b) cell dry mass concentration, denoted [X] ($g_{drycell}$ L^{-1}). Each marker represents an independent assay. A corresponds to the first test and D and E to the last ones.

intracellular cell compounds released after cell lysis could be used by the surviving bacteria to build up enzymes able to transform the substrates available in the reaction medium [46]. Cell lysis is thus assumed to play a key role for the bacteria to adapt their enzymatic machinery to their new CO_2 substrate and express the CO_2-reducing enzymatic system.

The different ^{13}C-formate concentration profiles observed between trials suggested a difference in the expression level by the bacteria of the enzymatic system reducing CO_2 and/or in the specific activity of this enzymatic system. For all tests, an acidification of the reaction medium was observed leading to a pH decrease from 7.0 ± 0.1 to a value around 6.4 ± 0.2 over the first five days before remaining quasi-constant up to 35 days (data not shown); this pH value corresponding to the pKa of the couple CO_2, H_2O/HCO_3^- (*i.e.* 6.4). pH was therefore not the cause of these differences. Preservation methods of the strain could be at the origin of the variations evidenced between experiments. Sub-cultures on LB agar medium were made between run A and B, and between run C and runs D-E. All these sub-cultivation steps led to a reduction in the latency period between two consecutive runs and thus ^{13}C-formate productivity (Fig. 2a). This observation is consistent with the fact that carrying out successive liquid cultures might contribute to enhancing the enzymatic activity of the cells and/or inducing strain evolution, improving adaptation to new conditions [46]. In contrast, the formate productivity dropped between kinetics B and C, *i.e.* after bacteria freezing (Fig. 2a). It is likely that the freezing storage step between these two runs caused damage to the cell components. Studies focused on bacteria freezing showed that this preservation method can have a significant effect on viability, autolytic activity and intracellular enzymatic activity [47]. Freezing could therefore have an influence on the bacterial CO_2-reducing activity of the cells.

$^{13}CO_2$ reduction assays were also carried out in batch mode with the commercial *S. maltophilia* strain (NCIMB 9203) that was delivered as a pure culture. The isolated strain was tested in parallel in the same conditions and notably at the same initial mass concentration (3.1 ± 0.2 $g_{dry\ cell}\ L^{-1}$). Table 1 gives the initial and final dry cell mass concentration [X] ($g_{dry\ cell}\ L^{-1}$) and the ^{13}C-formate concentration [^{13}C-formate] (μmol L^{-1}).

Both strains showed the same behavior for biomass concentration (Table 1) and for pH with a quick stabilization of CO_2, H_2O/HCO_3^- pKa (data not shown). The two strains also exhibited ^{13}C-formate production. However, the commercial strain resulted in the highest final ^{13}C-formate concentration with an identical biomass decrease throughout the reaction (Table 1) and consequently the best specific activity. This phenomenon might be explained by the fact that the commercial bacterium was never frozen and always kept as a pure culture.

In these exploratory and preliminary results, whole cells of *S. maltophilia* NCIMB 9203 (either isolated or purchased) were therefore demonstrated to reduce $^{13}CO_2$ into ^{13}C-formate ($H^{13}COO^-$) in batch mode. The balance describing such a reduction reaction is given by Eq. (3):

$$^{13}CO_2 + H^+ + 2e^- \rightarrow H^{13}COO^- \quad (3)$$

where H^+ designates protons and e^- electrons.

For all runs, the ^{13}C-formate concentrations produced were however much lower than the theoretical maximal concentration, *i.e.* 112.5 mmol L^{-1} (assuming that one mole of introduced $^{13}CO_2$ gave one mole of $H^{13}COO^-$), which suggests that there was no $^{13}CO_2$ limitation. On the contrary, the ability of the strain to express the enzymes required to catalyze CO_2 reduction as well as limitations of protons and electrons involved in the reaction (see Eq. (3)), were suspected to have an influence on the specific CO_2-reducing activity of the cells. To confirm these assumptions, the effect of the initial bacterial concentration and the addition in the reaction medium of a compound likely to serve as electron and proton donors, were investigated.

Table 1
$^{13}CO_2$ reduction trials in batch mode carried out with the isolated and the commercial strains of *S. maltophilia* (NCIMB 9203).

	[X] $g_{dry\ cell}\ L^{-1}$		[^{13}C-formate] μmol L^{-1}	
	0 day	35 days	0 day	35 days
Isolated strain	3.3 ± 0.1	0.6 ± 0.1	0	50 ± 5
Commercial strain	3.1 ± 0.2	0.6 ± 0.1	0	280 ± 10

Influence of the initial bacterial concentration

In previous experiments, the initial mass concentration of the bacterial suspension used for the $^{13}CO_2$ reduction tests was set at 3.1 ± 0.2 $g_{dry\ cell}\ L^{-1}$. A lower concentration (1.6 ± 0.1 $g_{dry\ cell}\ L^{-1}$) of the same stock of bacterial suspension was tested to investigate whether the quantity of ^{13}C-formate produced correlated with the initial cell quantity; the other reaction parameters remaining unchanged. The kinetics were monitored over 25 days. Table 2 summarizes the results obtained.

Table 2 shows that the final ^{13}C-formate concentration is nearly 20 times higher when the initial bacterial concentration is doubled. Contrary to what might be expected, the final concentration accumulated in ^{13}C-formate is therefore not correlated with the cell quantities introduced initially. Furthermore, it is interesting to note that by doubling the initial bacteria quantity, the final quantity of lysed cells is nearly also doubled (Table 2, Δ[X]). The compounds released in the reaction medium by cell lysis could consequently be used by the surviving cells to produce a greater quantity of intracellular enzymes reducing CO_2, which could induce a significant increase of the bacterial specific activity and thus a much greater ^{13}C- formate production. In conclusion, the availability of intracellular compounds in the reaction medium seems to be a limiting factor for CO_2 reduction performance when the initial bacterial concentration is low (1.6 $g_{dry\ cell}\ L^{-1}$).

Addition of a potential electron and proton donor in the reaction medium

Poly-3-HydroxyButyrate (PHB), a known energy storage lipid that can accumulate in the bacterial cells, was first tested as an electron and proton donor. Some strains of *S. maltophilia* have been reported to produce PHB [48]. PHB can notably be depolymerized into a 3-hydroxybutyrate monomer that acts as the source of electrons and protons [49] when oxidized into acetoacetate. PHB is a polymer with a high molecular weight that is insoluble in water, making its transport through the cell walls in its polymerized form impossible. Nevertheless, the *S. maltophilia* strain possesses the ability to excrete some extracellular PHB-depolymerases that hydrolyzes PHB into its water-soluble monomer which can enter the cells and be assimilated [49]. Addition of PHB was thus tested in the reference reaction medium and the ^{13}C-formate production was assessed throughout the reaction. For each trial, a reference (*i.e.* without PHB doping) was simultaneously monitored to analyze the effect of PHB addition.

An initial intracellular PHB mass content of 1.0 ± 0.1% *w/w* was measured, corresponding to a PHB concentration of 30 ± 2 mg L^{-1} - since the initial biomass concentration was fixed at 3.1 ± 0.2 $g_{dry\ cell}\ L^{-1}$. Such a PHB mass content was reported to be usual in *S. maltophilia* species [48]. PHB was therefore added at a final concentration of 300 mg L^{-1} to be in significant excess compared to the native

Table 2
$^{13}CO_2$ reduction trials carried out in batch mode: initial [X_0] and final [X_f] biomass concentrations (in $g_{dry\ cell}\ L^{-1}$), biomass loss Δ[X] at the end of the reaction (in %) and final concentrations of ^{13}C-formate [^{13}C-formate]$_f$ accumulated in the reaction medium due to $^{13}CO_2$ reduction (μmol L^{-1}).

[X_0] $g_{dry\ cell}\ L^{-1}$	[X_f] $g_{dry\ cell}\ L^{-1}$	Δ[X]%	[^{13}C-formate]$_f$ μmol L^{-1}
3.1 ± 0.2	1.1	65	650 ± 30
1.6 ± 0.1	0.7	56	30 ± 2

intracellular PHB stock in the *S. maltophilia* population.

Two independent series were launched, *i.e.* from two different bacterial cultures. Sampling was undertaken up to 20 days for the first series, and up to 35 days for the second. The ^{13}C-formate produced was measured for the whole suspension throughout the kinetics. The intracellular PHB concentration was also monitored in the bacterial pellets in reference conditions. However, due to the low solubility of PHB in water, its concentration could not be estimated in the reaction medium.

In all series, production of ^{13}C-formate was much higher when PHB was added to the reaction medium (Fig. 3). The production in presence of PHB was indeed at least tripled compared to the reference conditions (Fig. 3, series (1) at 20 days), and a maximal ^{13}C-formate production of 660 μmol L^{-1} was reached after 35 days of reaction with PHB addition (Fig. 3, series (2)). Regarding the kinetics (Fig. 3), the production of ^{13}C-formate always appeared significantly earlier when PHB was added. Also, in reference conditions, PHB content decreased (from 30 ± 2 mg L^{-1} to about 13 ± 1 mg L^{-1} from day 20) and then remained constant to a concentration that might be a minimal concentration regulated by the bacteria. These results tend to shows that PHB is a limiting factor and suggests it could be a direct electron and proton source for CO_2 reduction catalyzed by *S. maltophilia.* However, it cannot be excluded that PHB could also be used as a carbon and energy source for the bacteria to maintain and adapt their biological activities. Unfortunately, addition of PHB (insoluble in water) in the PHB series made optical density measurements impossible to conclude on possible bacterial growth or biomass stagnation during reaction.

Intensification of the CO_2-reducing bioprocess in a fed-batch electrolyzer

According to Section 4 of the Results, the CO_2 reduction reaction was probably limited by the intracellular quantity of electron and proton donors such as PHB. *S. maltophilia* was already reported to be electroactive for oxidation reactions [50–52], *i.e.* able to exchange electrons with a polarized anode – if the electrode potential and material make these reactions thermodynamically and kinetically possible. *S. maltophilia* was implemented in an electrolysis reactor where an infinite source of electrons could be provided by a polarized cathode in order to intensify the reduction reaction.

The electrolyzer was composed of three electrodes: (i) a polarized cathode (location of the reduction reaction) whose role was to provide the electrons, (ii) an Ag/AgCl reference electrode enabling a constant potential at the cathode and (iii) a counter-electrode (anode) allowing on the one hand the passage of the current and on the other hand the production of protons necessary for the reduction reaction. Continuous feeding of CO_2 was maintained in the reactor to (i) ensure deoxygenation of the bacterial suspension in RM and avoid competition with the aerobic metabolic pathway (where O_2 would become the final electron acceptor instead of CO_2) and to (ii) avoid CO_2 limitation due to the

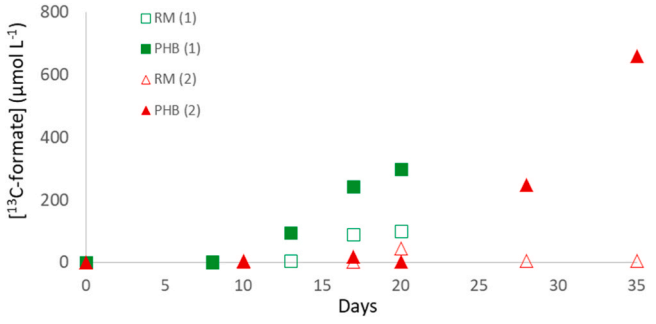

Fig. 3. $^{13}CO_2$ reduction trials carried out in batch mode: evolution of the ^{13}C-formate concentration for the reaction medium enriched with PHB (PHB) and the reference reaction medium (RM); two independent series were carried out, (1) and (2) respectively.

reducing activity of the *S. maltophilia* bacterium. Alternatively, CO_2 feeding was replaced by continuous argon bubbling to assess the CO_2 dependence of the electrochemical reactor. A chrono-amperometry analysis of the system giving the current I (A) versus time was carried out for the different conditions tested. In this work, current I was reported for the projected active cathode area, expressed in current density j (A m^{-2}). Six independent tests were carried out and one of these tests is presented in Fig. 4.

By convention, positive currents at the working electrode are linked to oxidation reactions while negative currents revealed reduction reactions; the more negative the reduction currents, the greater the reduction currents. Fig. 4 shows the evolution of the current measured over time in one of the bio-electrolyzers implemented with *S. maltophilia* for CO_2 reduction. This feasibility trial was carried out with a polarization potential of - 0.7 V *vs* Ag/AgCl to avoid water reduction - and thus the production of H_2 - occurring.

The current oscillated around 0.0 ± 0.01 A m^{-2} over the first 24 h, which corresponds to the signal baseline. This demonstrates that the compounds present initially in the bacterial suspension were not significantly reduced or oxidized (Fig. 4 A). A small current reduction appeared after 1.2 days (up to −0.2 A m^{-2}). However, this current returned to baseline before a significant reduction current appeared from the second day, reaching a stabilized value of - 1.4 A m^{-2} (Fig. 4 A). The current profile exhibited a shape usually encountered for microbial growth kinetics, suggesting the establishment of reduction reactions catalyzed by the bacteria. A control reactor launched over 11 days without bacteria showed that the current reduction did not exceed - 0.04 A m^{-2} (data not shown), which confirmed the role of bacteria in the increase of current reduction (Fig. 4 A).

In order to assess experimentally if the current reduction observed was linked to CO_2, CO_2 bubbling was replaced by argon (Ar) bubbling. Argon is an inert gas that could drive out the dissolved CO_2. Argon bubbling was initially carried out at a flow rate of 10 mL min^{-1} for 3 hours and the current decreased by a factor of nearly 2 (*i.e.* from - 1.40 to - 0.80 A·m^{-2}, Fig. 4 A and 4B). Then, the gas bubbling was cut off and the current reduction did not vary significantly, staying at around – 0.80 A m^{-2} (Fig. 4 C). The consistency of the current reduction could be due to the presence of CO_2 residue in the bacterial suspension; indeed, CO_2 is highly soluble in water and the argon flow rate that was implemented was possibly too weak to remove all CO_2 traces during this time.

A CO_2 flow rate was then reapplied at 10 mL min^{-1} and the reduction current increased again (Fig. 4D) until it reached the stabilized value observed at the end of the first CO_2 bubbling, *i.e.* - 1.4 A m^{-2} (Fig. 4 A and 4D). These elements suggest that the reduction current is driven by the CO_2 availability in the system.

Finally, a high argon flow (100 mL min^{-1}) was applied for 3 h, which made the current instantaneously rise up to nearly 0 A m^{-2} (Fig. 4E). At the same time, pH passed from 6.4 ± 0.1–7.2 ± 0.1, which could only induce a maximum potential shift of 0.05 V (*i.e.* - 0.060 x ΔpH at 30°C) on the redox potentials depending on pH, such as water. The pH change was thus not expected to have significant impact on the reduction reactions occurring at this potential. Consequently, a zero-current means that no - or insignificant - reduction reaction took place at the cathode when CO_2 was absent from the reaction medium, and that water was not reduced into H_2 in these conditions.

The current then increased when a CO_2 flux was applied again, and achieved a significant current of approximately - 0.3 A m^{-2} after 1 day (Fig. 4 F). These results suggest that CO_2 is the final electron acceptor reduced by *S. maltophilia* at the cathode. Reproducibility studies confirmed that the CO_2-reduction current returned to its stabilized value after alternating CO_2 removing (by argon flush) and re-bubbling at polarization potentials fixed either at −0.7 V or −0.8 V *vs* Ag/AgCl. These studies also highlighted stable CO_2-reduction currents up to 46 days (data not shown). An example is given in Fig. 5.

When CO_2 was fed at 10 mL min^{-1}, a stable reduction of about −0.25 A m^{-2} was reached (Fig. 5A). The current reduced to almost zero

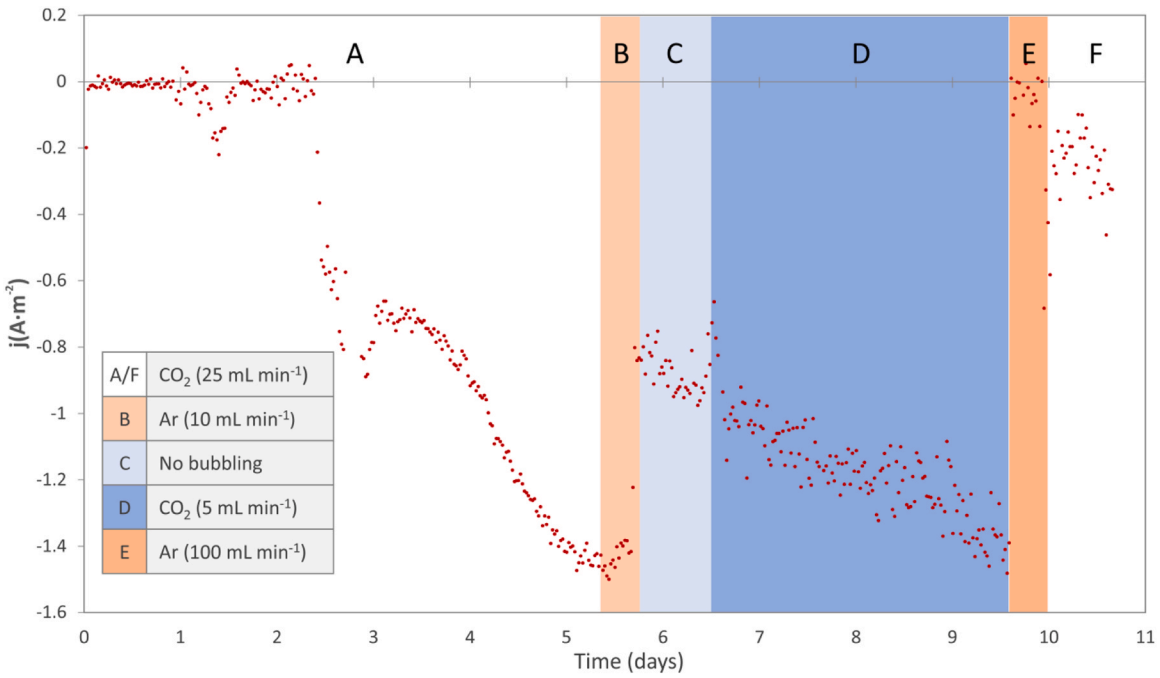

Fig. 4. $^{13}CO_2$ reduction in a 100 mL-fed-batch electrolyzer inoculated with *S. maltophilia*: chronoamperogram (CA) obtained on a cathode polarized at – 0.7 V vs Ag/AgCl. Six phases are distinguished, corresponding to the different operating conditions implemented: (A) CO_2 bubbling (25 mL min^{-1}); (B) Argon (Ar) bubbling (10 mL min^{-1}); (C) stop of the gas bubbling; (D) CO_2 bubbling (5 mL min^{-1}); (E) Argon bubbling (100 mL min^{-1}) and (F) CO_2 bubbling (25 mL min^{-1}).

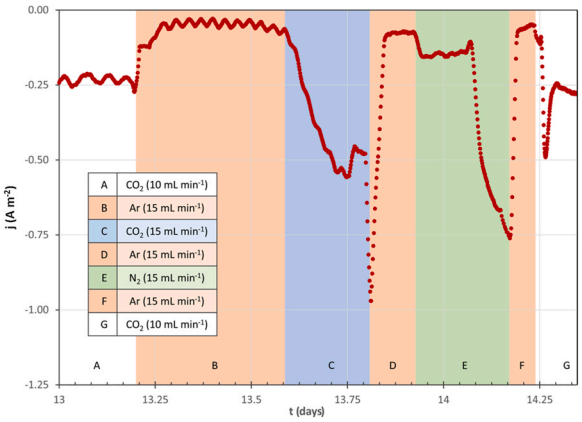

Fig. 5. $^{13}CO_2$ and N_2 reduction tests in a fed-batch electrolyzer inoculated with *S. maltophilia*: chronoamperogram (CA) obtained on a cathode polarized at – 0.8 V vs Ag/AgCl after 14.5 days – the reduction current having occurred from day 7. Seven phases were distinguished, corresponding to the different operating conditions implemented: (A) CO_2 bubbling (10 mL min^{-1}); (B) Argon (Ar) bubbling (15 mL min^{-1}); (C) CO_2 bubbling (15 mL min^{-1}); (D) Argon (Ar) bubbling (15 mL min^{-1}); (E) N_2 bubbling (15 mL min^{-1}); (F) Ar bubbling (15 mL min^{-1}); and (G) CO_2 bubbling (10 mL min^{-1}).

when CO_2 was removed from the reaction medium containing the bacteria (*i.e.* after argon bubbling, Fig. 5B); the very slight current that remained (about – 0.02 to – 0.04 A m^{-2}) being possibly due to restrained proton reduction into H_2 at −0.8 V *vs* Ag/AgCl. When CO_2 was fed again at a higher flow rate of 15 mL min^{-1} (Fig. 5C), the current increased, to stabilize at a higher value (*i.e.* −0.5 A m^{-2}) than obtained before argon bubbling (Fig. 5A and B), suggesting a CO_2 limitation and the potential for higher current values at higher CO_2 flow rates. An argon flow was then supplied to remove CO_2 from the reaction medium and the current returned to near zero (Fig. 5D). This result confirms that the reduction current observed is driven by CO_2.

Both isolated and purchased *S. maltophilia* were tested in bio-electrolyzers and exhibited similar electro-activities. In conclusion, *S. maltophilia* was shown to catalyze the reduction of CO_2 in a fed-bath electrolyzer where electrons and protons can be directly fed by the cathode and are unlimited.

To quantify the ability of *S. maltophilia* to remove CO_2, an identical mixture of CO_2/Ar 1:1 *v/v* (where argon served as an internal standard) was flowed through 5 independent bio-electrolyzers and their associated blank reactors (bio-electrolyzer without bacteria). CO_2 content was analyzed at the gas outlets of these reactors to get the CO_2 removals, by comparison to the blank. These removals were defined as the ratio of the quantity of CO_2 consumed in the reactor to the quantity having passed across the reactor - for the fed-batch mode - or initially present - for the batch mode. Removals ranging from 5 and to 25% *v/v* were reached in the bio-electrolyzers, depending on the initial bacterial physiology, the experiment duration or the CO_2 rate (*i.e.* the CO_2 volume fed per volume of bacteria suspension per minute, in min^{-1}). The best result (*i.e.* 25% CO_2 removal) was obtained with bacteria that were preserved on plates at 4°C (*i.e.* by plate sub-cultures every two weeks for 6 months at a maximum), after at least 15 days of experiment and with a CO_2 rate of 0.19 min^{-1}.

Comparison between the different operating modes: batch, fed-batch and fed-batch electrolyzer (i.e. bio-electrolyzer)

It is worth noting that the lowest removal measured in the fed-batch electrolyzers (*i.e.* 5%) was at least 20-times higher than the best levels obtained in batch reactors. This result demonstrates the beneficial impact of the bio-electrolyzer configuration on CO_2 reduction catalyzed by *S. maltophilia*. To distinguish the role of the fed-batch feeding to the electrodes in the bio-electrolyzer, three bioreactors were carried out in fed-batch mode without an electrode but in the same conditions as for the bio-electrolyzers. These experiments showed that the fed-batch mode without electrodes noticeably improved (by 10-fold on average) the CO_2 removal compared to the batch, probably thanks to the enhancement of the CO_2 transfer that it permitted. In fed-batch mode, the concentration of soluble CO_2 available for the bacteria is indeed likely to be significantly higher than in batch mode which could increase

the CO_2 reduction rate. Similarly to the batch mode, cell lysis occurred in the fed-batch bioreactor since the OD_{600} of the bacterial suspensions went from 6.0 ± 0.2 on average at the beginning of the experiment to 2.2 ± 0.2 at the end (46 days at a maximum). As seen previously (Results, Sections 2 and 3), the cellular compounds released in the reaction medium due to cell lysis might be used by the cells to adapt their enzymatic machinery but also to renew its electron donor stock, such as PHB (Fig. 6A).

Besides, it appeared that the presence of the electrodes increased by at least 2-times the CO_2 removal compared to the sole fed-batch. This result is probably explained by the electron feeding allowed by the polarized cathode that was shown by the appearance of a reduction current (see Results, Section 5). Bio-electrolysis was therefore assumed. In bio-electrolysis [53,54], the electrons and protons provided by the electrodes are expected to be used directly by the intracellular enzymatic system catalyzing the CO_2 reduction reaction (Fig. 6B). The continuous flow of electrons and protons is intended to replace the electrons and protons coming from the intracellular donors like could be PHB (Fig. 6B). The product of CO_2 reduction in presence of electrodes has not yet been identified (assumed formate, Figs. 6B and 6C). However, the Faraday law application - based on the currents and times measured in the bio-electrolyzer - gave a maximal theoretical CO_2 removal (by considering 2 electrons exchanged during CO_2 reduction) that is at least 20-times smaller than the experimental CO_2 removals measured. This observation suggests that bio-electrolysis is not the only phenomenon occurring in the bio-electrolyzers; otherwise, the measured and calculated CO_2 removal would have been of the same order of magnitude. Electro-fermentation was therefore suspected. In electro-fermentation [53,54], electrical energy would no longer be the predominant energy source since the protons and electrons would be directed to maintenance processes, for example for producing PHB (Fig. 6C). The intracellular PHB produced would then be almost entirely devoted to reducing CO_2, becoming the main energy source for the reduction reaction. In such configuration, the overall energy demand would be consequently lower compared to a CO_2 electrolysis process and Faraday's law would no longer correlate the reduction current with the removed CO_2 content.

Trials to approach the intracellular enzymatic system catalyzing CO_2 reduction in S. maltophilia

In batch mode, the enzyme catalyzing CO_2 reduction in *S. maltophilia* was demonstrated to reduce CO_2 into formate without requiring H_2 (Results, Section 2 and Fig. 6A). Formate dehydrogenase (FDH) is a

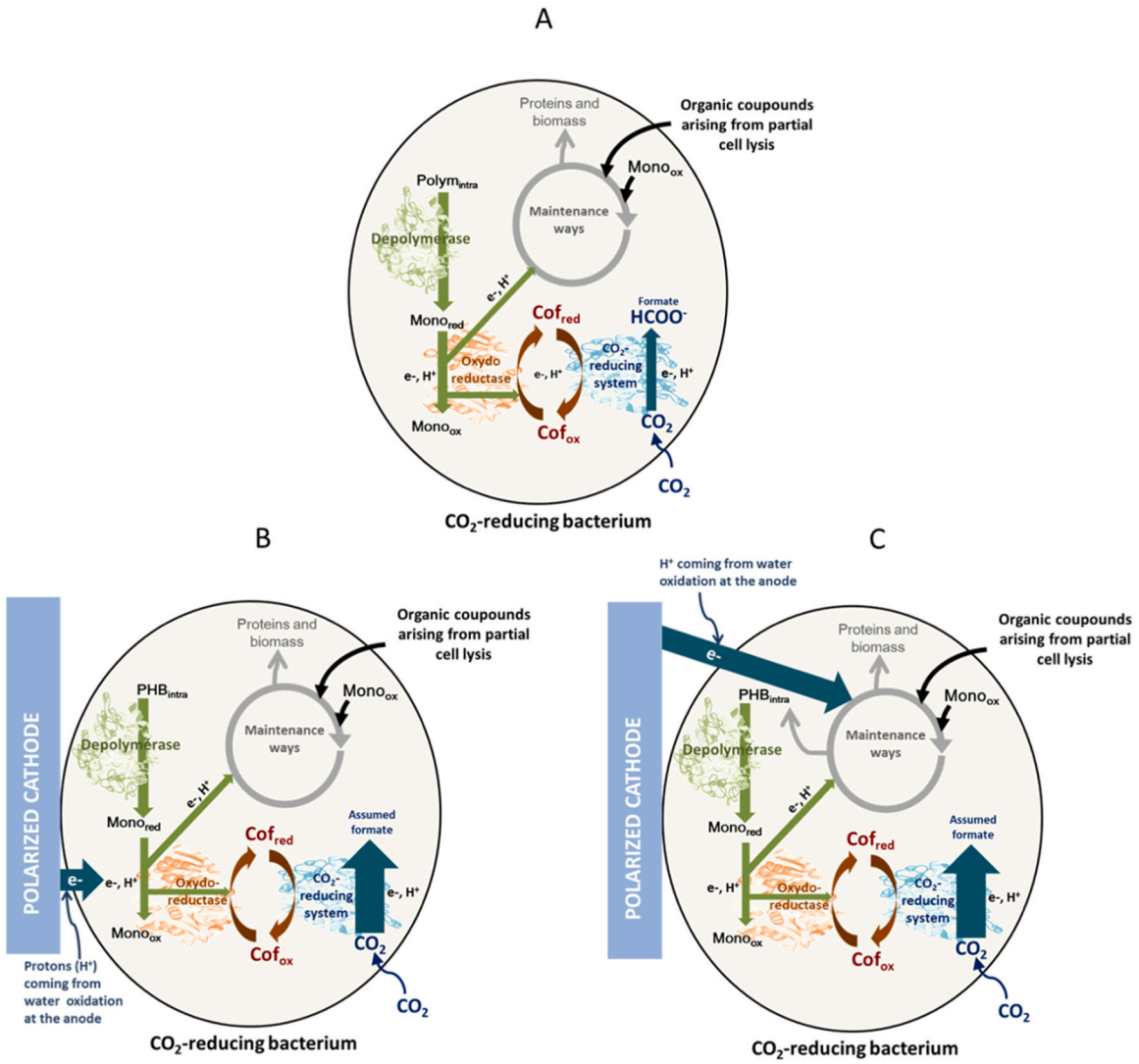

Fig. 6. Assumed mechanisms (A) in batch and fed-batch modes and in bio-electrolyzer mode with (B) bio-electrolysis and (C) electro-fermentation phenomena. PHB means PolyHydroxyButyrate. $Mono_{red}$ is the reduced form of the PHB monomer, *i.e.* 3-hydroxybutyrate. Monoox is the oxidized form of Monored, *i.e.* acetoacetate. $Cofr_{ed}$ and Cof_{ox} designates the cofactor of the CO_2-reducing enzymatic system (currently unkown), in its reduced and oxidized form, respectively.

common bacterial enzyme reported to be reversible and able to catalyze the reduction of CO_2 into formate [21,22]. It is consequently suspected that this is involved in the current bioprocess. However, nitrogenases are also described in the literature as reducing CO_2 [23]. Given that nitrogen (N_2) is the natural substrate of nitrogenases, tests were carried out in batch mode with or without N_2 to identify a possible nitrogenase activity. Three conditions were assayed (with a same bacterial suspension): $^{13}CO_2$/air 3:7 *v/v*, $^{13}CO_2/N_2$ 3:7 *v/v* and $^{13}CO_2$. If there is an active nitrogenase, the N_2 present in the reactor could be reduced into ammonia and finally into ammonium ions (NH_4^+) since the pH was buffered at 6.4. The ammonium concentration was monitored, as ^{13}C-formate, throughout the kinetics. The kinetics were performed over 31 days. Table 3 summarizes the results obtained.

Whatever the conditions tested, the ^{13}C-formate concentrations accumulated in the reactors were the same, *i.e.* 90 ± 10 μmol L^{-1} (Table 3). Ammonium ions were produced in significant quantities when $^{13}CO_2$ was pure, *i.e.* 3.0 ± 0.5 mmol L^{-1} (Table 3). Since there was no N_2 in the batch headspace, N_2 reduction was impossible. The presence of NH_4^+ could then be explained by a deamination of the proteins [43] released in the suspension after partial cell lysis, as already evidenced in Results, Section 2, with OD_{600} having decreased from 10.0 ± 0.2–2.0 ± 0.5. For the mixture containing $^{13}CO_2$ and N_2 ($^{13}CO_2/N_2$, 3:7 v/v), NH^{4+} production was almost double in comparison to $^{13}CO_2$ alone (Table 3). This result suggests that another phenomenon was taking place. The presence of an active nitrogenase inside the cells catalyzing N_2 reduction into NH_4^+ could explain this. When N_2 was introduced in the reactor, both N_2 reduction by nitrogenase and amino acid degradation could indeed occur at the same time. When O_2 was also initially present in the reactor headspace ($^{13}CO_2$/air 3:7 *v/v*), NH_4^+ production was expected to be lower since O_2 is known to be an inhibitor of the nitrogenases [55]. However, NH_4^+ production once again nearly doubled compared to the $^{13}CO_2/N_2$ mixture (Table 3). Consequently, the increase of NH_4^+ may result from the degradation of the proteins released through metabolic pathways favored by the presence of O_2. Nevertheless, the activity of a potential nitrogenase was also not excluded after 14 days of reaction. NH_4^+ ions were indeed still produced after 14 days of reaction, whereas O_2 became zero (data not shown).

In order to check the possible N_2 reduction into NH_4^+ by *S. maltophilia*, a fed-batch electrolyzer was fed with N_2 and argon after bacteria accommodation to CO_2 (Fig. 5 A to D). As previously observed, when the reactor was fed with argon (Fig. 5D), the current was almost zero. But when N_2 was bubbled, a N_2-reduction current immediately occurred (Fig. 5E). This current remained at a low value (about -0.15 A m^{-2}) for 0.2 days before the current increased to reach a significantly higher value (- 0.8 A m^{-2}) than the maximum observed with CO_2 bubbling, *i.e.* -0.6 A m^{-2} (Fig. 5 C). The transitory period observed could be linked to the time required to saturate the reaction medium with N_2 (since N_2 is poorly soluble in water) and to adapt *S. maltophilia* to N_2. Argon was then bubbled and the current dropped to zero (Fig. 5 F), which revealed an N_2-dependant reduction current (Fig. 5E). Finally, CO_2 was fed again at 10 mL min^{-1} and the current then increased and stabilized at a value similar to that obtained under the same conditions (Fig. 5 A and 5 G). This suggests that N_2 supply did not damage the enzymatic system in charge of CO_2 reduction.

Table 3
$^{13}CO_2$ reduction trials carried out in batch mode with different initial gaseous mixtures: initial and final concentrations of NH_4^+ ([NH_4^+], mmol L^{-1}) and ^{13}C-formate ([^{13}C-formate], μmol L^{-1}).

	[^{13}C-formate] μmol L^{-1}		[NH_4^+] μmol L^{-1}	
Gaseous mixtures	0 day	31 days	0 day	31 days
$^{13}CO_2$/air 3:7 *v/v*	0	90 ± 10	0.2 ± 0.1	10 ± 2
$^{13}CO_2/N_2$ 3:7 *v/v*	0	90 ± 10	0.2 ± 0.1	5.5 ± 0.3
$^{13}CO_2$	0	90 ± 10	0.2 ± 0.1	3.0 ± 0.5

N_2 was consequently assumed to be reduced by *S. maltophilia* at the cathode, which reinforces the hypothesis of a possible reduction of N_2 in the batch reactor. The polarization of the cathode at - 0.8 V *vs* Ag/AgCl makes this reaction thermodynamically possible since the redox potential of the couple N_2/NH_4^+ is - 0.35 V *vs* Ag/AgCl at pH 6.4 [56]. The adaptation time of *S. maltophilia* to N_2 substrate was significantly shorter in comparison to CO_2 (*i.e.* 0.2 days *vs* 7 days). The same enzyme was therefore assumed to catalyze both reduction reactions (*i.e.* N_2 and CO_2 reductions) with nitrogenase probably being the intracellular enzyme enabling these two reactions.

Genome sequencing analyses were carried out on the native S. *maltophilia* strain (post reaction). The sequencing resulted in a high-quality metagenome assembled genome (MAG) corresponding to *Stenotrophomonas maltophilia* (100% completion, 0% redundancy). To check the possible presence of FDH and nitrogenase enzymes in *S. maltophilia*, genes coding for a part of a known FDH (Mo, W, FeS, FMN or NAD) or a known nitrogenase (Fe, MoFe or VFe) were searched for in the genome of *S. maltophilia* MAG using the PFAM database. Results are reported in Table 4. Lowest e-values correspond to highest homologies and an e-value of zero means the probability of the enzyme gene to be coded is 100%. High homologies (*i.e.* low e-values) were found between the genome and the genes identified coding for both enzyme parts. The contribution of FeS-FDH and Fe-nitrogenase to CO_2 reduction is thus very likely (Table 4).

4. Conclusions

S. maltophilia, a native environmental bacterium, was shown to reduce CO_2. Formate was identified as the product of the CO_2 reduction reaction in batch mode. This new process is very promising as it works without H_2, cofactor or photon addition. The CO_2 reduction can be enhanced by PHB adding or in a fed-batch electrolyzer providing electrons and protons to the bacteria. Fed-batch electrolysis allowed CO_2 removals up to 25% *v/v* at 30°C and atmospheric pressure. *S. maltophilia* was also demonstrated to reduce N_2, which constitutes another exciting aspect of this work. Intracellular FeS-FDH and Fe-nitrogenase are currently assumed to be part of the mechanism. Further research, including reactor optimization and omics studies are expected to elucidate the detailed bacterium mechanism and intensify CO_2 reduction. Carbon balance on the overall process will also be carried out and trials to cultivate the bacterium on a renewable waste will be investigated.

CRediT authorship contribution statement

Djahida Benmeziane: Investigation, Methodology. **Eddy Petit:**

Table 4
Summary table of the genes found in *S. maltophilia* genome coding for parts of nitrogenase and FDH enzymes. The e-values and gene function are also detailed.

Gene	Function	e-value
Fer4-NifH	4Fe-4S iron sulfur cluster binding proteins, NifH/frxC family	1.80 10^{-11}
nifH	nitrogenase iron protein	3.50 10^{-12}
nifH	nitrogenase iron protein	1.40 10^{-12}
Fer4-NifH	4Fe-4S iron sulfur cluster binding proteins, NifH/frxC family	3.00 10^{-16}
NifU	NifU-like domain	6.8010^{-24}
fdh-trans	Formate dehydrogenase N, transmembrane	1.90 10^{-24}
fdh-gamma	formate dehydrogenase subunit gamma	2.2010^{-60}
fdhD-narQ	formate dehydrogenase accessory sulfurtransferase FdhD	4.90 10^{-67}
fdhE	formate dehydrogenase accessory protein FdhE	6.40 10^{-76}
fdh-beta	formate dehydrogenase FDH3 subunit beta	4.80 10^{-145}
fdh-alpha	formate dehydrogenase-N subunit alpha	0

Investigation. **Loubna Karfane:** Resources. **Héloïse Baldo:** Investigation. **Azariel Ruiz-Valencia:** Conceptualization, Investigation, Methodology, Validation, Writing – original draft, Writing – review & editing. **Louis Cornette de Saint Cyr:** Conceptualization, Investigation, Methodology, Validation, Writing – original draft, Writing – review & editing. **José Sanchez Marcano:** Conceptualization, Writing – review & editing. **Marie-Pierre Belleville:** Conceptualization, Writing – review & editing. **Laurence Soussan:** Conceptualization, Funding acquisition, Investigation, Methodology, Project administration, Supervision, Validation, Writing – original draft, Writing – review & editing. **Valérie Bonniol:** Investigation. **Sophie Pécastaings:** Investigation, Methodology, Writing – review & editing. **Christine Roques:** Investigation, Methodology, Writing – review & editing. **Delphine Paolucci-Jeanjean:** Writing – review & editing.

Declaration of Competing Interest

There are no conflicts of interest to declare.

Data Availability

Data will be made available on request.

Acknowledgements

Montpellier University and SATT axLR for funding. Genoscreen for 16 S RNA and genome sequencing. ACB&Co for having read and checked the English of the manuscript.

Appendix

Isolation and identification of S. maltophilia

An environmental consortium with *M. trichosporium* OB3b was previously obtained at our Laboratory, having showed that it reduced CO_2.[32] Isolation and identification of the strains forming this consortium were carried out. To facilitate the study, the consortium samples were inoculated on two heterotrophic media: Tryptic Soy Broth (TSB) and Lysogeny Broth (LB) Miller. These two standard media were ordered from Sigma (France) and differ in their NaCl concentrations (5 and 10 g L^{-1} respectively) and carbon sources (glucose *vs* yeast extract). These factors could indeed play a role in the strain differentiation. After incubation at 30°C in aerobic conditions, two consortia were obtained: consortium I (on TSB) and consortium II (on LB). These consortia were Gram stained and observed by microscopy.

Three bacteria were distinguished by microscopy in these consortia: (i) a small Gram-negative bacillus which was present and predominant, (ii) a small Gram-positive bacillus that was always present and (iii) a large Gram-negative bacillus that was visible sparingly in consortium I only. It is worth noticing that the methanotrophic bacterium *M. trichosporium* OB3b was not expected to be observed since the cultivation conditions did not match the necessary requirements (*i.e.* presence of methane in the gas in contact with the plates).

Bacteria were then isolated from consortia I and II by exposure to selective culture conditions. Colonies from the plates were recovered separately to inoculate both TSB and LB culture media; the inoculated media were then incubated in four different conditions: (i) 37°C in contact with air, (ii) 30°C in contact with air, (iii) 37°C in anaerobic conditions and (iv) 37°C in anaerobic conditions on media beforehand with addition, or not, of colistine (10 mg L^{-1}), an antibiotic inhibiting Gram positive bacteria growth. After isolation of the bacteria from the consortia, bacteria were identified with regards to macroscopic and microscopic characteristics and biochemical properties (oxidase, catalase). Finally, strains were identified at the species level by MALDI-TOF MS (Maldi Biotyper Microflex®, Bruker Daltonics, Bremen, Germany; IVD 7712) (score $\geq$2.0). Mass spectrometry results demonstrated that:

(i) The small Gram-negative bacillus observed predominantly in both consortia was the same bacterium, *i.e. Stenotrophomonas maltophilia* (match score of 2.21),
(ii) The small Gram-positive bacillus observed in both consortia was the same bacterium, *i.e. Microbacterium oxydans* (match score of 2.05),
(iii) The large and very sparse Gram-negative bacillus that was observed in consortium I only was *Pantoea agglomerans* (match score of 2.07).

Sequencing the 16 S RNA of the isolated *Stenotrophomonas maltophilia* that was already used for CO_2 reduction tests confirmed that the bacteria identified was *S. maltophilia* and the genome matched at 99.87% to the known strain of *S. maltophilia* NCIMB 9203 (Materials and Methods, Section 5.d).

References

[1] J.G. Canadell, P.M.S. Monteiro, M.H. Costa, L. Cotrim da Cunha, P.M. Cox, A.V. Eliseev, S. Henson, M. Ishii, S. Jaccard, C. Koven, A. Lohila, P.K. Patra, S. Piao, J. Rogelj, S. Syampungani, S. Zaehle, K. Zickfeld, Climate change 2021: The Physical Science Basis, Contrib. Work. Group I Sixth Assess. Rep. Intergov. Panel Clim. Change (2021) 673–816.
[2] J. Tollefson, Nature 562 (2018) 172–173.
[3] V. Rodin, J. Lindorfer, H. Boehm, L. Vieira, *J. CO_2 Util.* 41 (2020) 101219.
[4] M.A. Scibioh, B. Viswanathan, Carbon dioxide to chemicals and fuels, Elsevier, 2018.
[5] H. Mikulčić, I.R. Skov, D.F. Dominković, S.R.W. Alwi, Z.A. Manan, R. Tan, N. Duić, S.N.H. Mohamad, X. Wang, Renew. Sustain. Energy Rev. 114 (2019) 109338.
[6] E.I. Koytsoumpa, C. Bergins, E. Kakaras, J. Supercrit. Fluids 132 (2018) 3–16.
[7] Y. Xie, J. Liang, Y. Fu, J. Lin, H. Wang, S. Tu, J. Li, *J. CO_2 Util.* 32 (2019) 281–289.
[8] J. Ma, J. Chen, X. Geng, B. Alford, Z. Zhang, H. Xiao, J. Tong, F. Peng, Nucl. Anal. 2 (2023) 100063.
[9] D. Ewis, M. Arsalan, M. Khaled, D. Pant, M.M. Ba-Abbad, A. Amhamed, M.H. El-Naas, Sep. Purif. Technol. (2023) 123811.
[10] K. Wiranarongkorn, K. Eamsiri, Y.-S. Chen, A. Arpornwichanop, J. CO2 Util. 71 (2023) 102477.
[11] X. An, P. Wang, X. Ma, X. Du, X. Hao, Z. Yang, G. Guan, Carbon Resour. Convers. 6 (2) (2023) 85–97.
[12] S. Gu, A.N. Marianov, T. Lu, J. Zhong, Chem. Eng. J. 470 (2023) 144249.
[13] M. Sajna, S. Zavahir, A. Popelka, P. Kasak, A. Al-Sharshani, U. Onwusogh, M. Wang, H. Park, D. Han, J. Environ. Chem. Eng. 11 (5) (2023) 110467.
[14] K. Qi, Y. Zhang, N. Onofrio, E. Petit, X. Cui, J. Ma, J. Fan, H. Wu, W. Wang, J. Li, J. Liu, Y. Zhang, Y. Wang, G. Jia, J. Wu, L. Lajaunie, C. Salameh, D. Voiry, Nat. Catal. 6 (2023) 319–331.
[15] Z. He, J. Goulas, E. Parker, Y. Sun, X. Zhou, L. Fei, Catal. Today 409 (2023) 103–118.
[16] I. Som, M. Roy, J. Alloy. Compd. 918 (2022) 165533.
[17] W. Wang, L. Wang, W. Su, Y. Xing, *J. CO_2 Util.* 61 (2022) 102056.
[18] V.-C. Nguyen, D.B. Nimbalkar, V. Hoang Huong, Yuh-Lang Lee, H. Teng, J. Colloid Interface Sci. 649 (2023) 918–928.
[19] Y. Guo, X. Hong, Z. Chen, Y. Lv, J. Energy Chem. 80 (2023) 140–162.
[20] P. Chiranjeevi, M. Bulut, T. Breugelmans, S.A. Patil, D. Pant, Curr. Opin. Green Sustain. Chem. 16 (2019) 65–70.
[21] Z. Zhang, T. Vasiliu, F. Li, A. Laaksonen, X. Zhang, F. Mocci, X. Ji, *J. CO_2 Util.* 60 (2022) 101978.
[22] B. Hu, D.F. Harris, D.R. Dean, T.L. Liu, Z.-Y. Yang, L.C. Seefeldt, Bioelectrochemistry 120 (2018) 104–109.
[23] H. Salehizadeh, N. Yan, R. Farnood, Chem. Eng. J. 390 (2020) 124584.
[24] A. Nisar, S. Khan, M. Hameed, A. Nisar, H. Ahmad, S.A. Mehmood, Microbiol. Res. 251 (2021) 126813.
[25] P. Xu, J. Li, J. Qian, B. Wang, J. Liu, R. Xu, P. Chen, W. Zhou, Chemosphere 319 (2023) 137987.
[26] R. Tang, X. Yuan, J. Yang, Biotechnol. Adv. 67 (2023) 108183.
[27] J. Panich, B. Fong, S.W. Singer, Trends Biotechnol. 39 (4) (2021) 412–424.
[28] S.R. Kim, S.-J. Kim, S.-K. Kim, S.-O. Seo, S. Park, J. Shin, J.-S. Kim, B.-R. Park, Y.-S. Jin, P.-S. Chang, and others, Bioresour. Technol. 346 (2022) 126349.
[29] F. Leo, F.M. Schwarz, K. Schuchmann, V. Müller, Appl. Microbiol. Biotechnol. 105 (14-15) (2021) 5861–5872.
[30] L. Luan, X. Ji, B. Guo, J. Cai, W. Dong, Y. Huang, S. Zhang, Biotechnol. Adv. 63 (2023) 108098.
[31] L. Soussan, A. Ruiz-Valencia, D. Benmeziane, J. Sanchez-Marcano, M.-P. Belleville and D. Paolucci-Jeanjean, French pat., WO2019234344 1A, 2019.
[32] A. Ruiz-Valencia, D. Benmeziane, N. Pen, E. Petit, V. Bonniol, M. Belleville, D. Paolucci, J. Sanchez-Marcano, L. Soussan, Catal. Today 346 (2020) 106–111.
[33] G.M. Boratyn, C. Camacho, P.S. Cooper, G. Coulouris, A. Fong, N. Ma, T.L. Madden, W.T. Matten, S.D. McGinnis, Y. Merezhuk, Y. Raytselis, E. Sayers, T. Tao, J. Ye, I. Zaretskaya, Nucleic Acids Res. 41 (2013) W29–W33.
[34] A.E. Minoche, J.C. Dohm, H. Himmelbauer, Genome Biol. 12 (2011) 1–15.
[35] D. Li, C.-M. Liu, R. Luo, K. Sadakane, T.-W. Lam, Bioinformatics 31 (10) (2015) 1674–1676.

[36] B. Langmead, S.L. Salzberg, Nat. Methods 9 (4) (2012) 357–359.
[37] A.M. Eren, Ö.C. Esen, C. Quince, J.H. Vineis, H.G. Morrison, M.L. Sogin, T. O. Delmont, PeerJ 3 (2015) e1319.
[38] P.-A. Chaumeil, A.J. Mussig, P. Hugenholtz, D.H. Parks, Bioinformatics 36 (2020) 1925–1927.
[39] M. Kanehisa, S. Goto, Nucleic Acids Res. 28 (1) (2000) 27–30.
[40] J. Mistry, S. Chuguransky, L. Williams, M. Qureshi, G.A. Salazar, E.L. Sonnhammer, S.C. Tosatto, L. Paladin, S. Raj, L.J. Richardson, R.D. Finn, A. Bateman, Nucleic Acids Res. 49 (D1) (2021) D412–D419.
[41] M.Y. Galperin, Y.I. Wolf, K.S. Makarova, R. Vera Alvarez, D. Landsman, E. V. Koonin, Nucleic Acids Res. 49 (D1) (2021) D274–D281.
[42] A.J. Pieja, E.R. Sundstrom, C.S. Criddle, Appl. Environ. Microbiol. 77 (2011) 6012–6019.
[43] G. Braunegg, B. Sonnleitner, R. Lafferty, Eur. J. Appl. Microbiol. Biotechnol. 6 (1) (1978) 29–37.
[44] H.R. Wallage, J.H. Watterson, J. Anal. Toxicol. 32 (3) (2008) 241–247.
[45] O. Mahdi, B. Eklund, N. Fisher, Curr. Protoc. Microbiol. 32 (2014) 6F–10F.
[46] J.M. Navarro Llorens, A. Tormo, E. Martínez-García, FEMS Microbiol. Rev. 34 (4) (2010) 476–495.
[47] S. Kandil, M. El Soda, Adv. Microbiol. 5 (6) (2015) 371–382.
[48] P. Singh, N. Parmar, Afr. J. Biotechnol. 10 (2011) 4907–4919.
[49] B. Tiwari, N. Manickam, S. Kumari, A. Tiwari, Bioresour. Technol. 216 (2016) 1102–1105.
[50] K. Venkidusamy, M. Megharaj, Front. Microbiol. 7 (2016) 1965.
[51] H. Xue, P. Zhou, L. Huang, X. Quan, J. Yuan, Sens. Actuators B: Chem. 243 (2017) 303–310.
[52] J. Shen, L. Huang, P. Zhou, X. Quan, G.L. Puma, Bioelectrochemistry 114 (2017) 1–7.
[53] R. Moscoviz, J. Toledo-Alarcón, E. Trably, N. Bernet, Trends Biotechnol. 34 (2016) 856–865.
[54] S.V. Mohan, S. Varjani, A. Pandey, Biomass, Biofuels, Biochemicals, in: S. V. Mohan, S. Varjani, A. Pandey (Eds.), Part I: Microbial Electrochemical Technology (Met) - Basics, Elsevier, 2018, pp. 3–224.
[55] H. Bladen, M. Bryant, R. Doetsch, Appl. Microbiol. 9 (2) (1961) 175–180.
[56] P. Vanysek, CRC Handbook of Chemistry and Physics, CRC Press, D.L. Ride, 2000, pp. 5–80 (Electrochemical series).